Detecting Emergent Continuous Symmetries at Quantum Criticality

Mingru Yang,[1] Bram Vanhecke,[1] and Norbert Schuch[1,2]
[1]University of Vienna, Faculty of Physics, Boltzmanngasse 5, 1090 Wien, Austria
[2]University of Vienna, Faculty of Mathematics, Oskar-Morgenstern-Platz 1, 1090 Wien, Austria

(Received 3 January 2023; accepted 23 June 2023; published 21 July 2023)

New or enlarged symmetries can emerge at the low-energy spectrum of a Hamiltonian that does not possess the symmetries, if the symmetry breaking terms in the Hamiltonian are irrelevant under the renormalization group flow. We propose a tensor network based algorithm to numerically extract lattice operator approximation of the emergent conserved currents from the ground state of any quantum spin chains, without the necessity to have prior knowledge about its low-energy effective field theory. Our results for the spin-1/2 J-Q Heisenberg chain and a one-dimensional version of the deconfined quantum critical points demonstrate the power of our method to obtain the emergent lattice Kac-Moody generators. It can also be viewed as a way to find the local integrals of motion of an integrable model and the local parent Hamiltonian of a critical gapless ground state.

DOI: 10.1103/PhysRevLett.131.036505

Introduction.—Low-energy physics can show different symmetries from the Hamiltonian. In the thermodynamic limit, the continuous symmetry of a Hamiltonian can be spontaneously broken in its ground state, or new symmetries that the Hamiltonian does not possess can *emerge* in its low-energy spectrum. The latter phenomenon of emergent symmetries is prevalent at the critical point of many quantum and classical phase transitions, provided the symmetry breaking terms in the Hamiltonian are irrelevant under the renormalization group (RG) flow. The most prominent example might be the deconfined quantum critical point (DQCP) [1,2], a direct continuous phase transition between two distinct spontaneous symmetry broken phases without fine-tuning, beyond the Landau-Ginzburg-Wilson paradigm. The emergent symmetry which reconciles the incompatible order parameters thus becomes the smoking gun to determine whether such a phase transition is really a DQCP. Another example is the extended symmetry in the low-energy eigenstates of a one-dimensional (1D) critical Hamiltonian with an internal semisimple Lie group symmetry, when its low-energy physics is described by a conformal field theory (CFT) [3,4]. In this case, the microscopic symmetry and the emergent symmetries can be recombined to form two independent symmetries acting, respectively, on the left- and right-moving fields, with the corresponding conserved charges being the zero modes of the Kac-Moody algebra [5,6].

Plenty of numerical efforts [7–10] have been devoted to confirming the existence of emergent symmetries. In the case of DQCP, the identity between the scaling dimensions of the critical fluctuations related by emergent symmetries would be an indication [8,11]. Other approaches include order parameter histograms [11,12] and level-crossing analysis [13]. A more direct probe of emergent symmetries is to check if the scaling dimensions of the effective lattice operators for the conserved currents in the field theory are equal to the space dimension [8,9]. However, identification of lattice operators to the currents in the continuum limit requires involved field theory and symmetry analysis [8,14]. Moreover, the identification is usually only approximate and also not unique.

Instead, tensor networks [15–18] provide us with much more information than simply a measurement outcome of the correlation function for given operators. In fact, rather than derive from field theory analysis, we are able to read out the lattice operator for the emergent conserved currents from a tensor network state in a straightforward way. Upon feeding a variationally optimized tensor network ground state [19,20], our algorithm returns the optimal lattice approximation of the conserved current operators truncated to a given interaction range N, which systematically approximates the exact symmetry generators as N increases.

Algorithm.—If a state $|\psi\rangle$ is symmetric under a global continuous symmetry transformation $U = e^{i\epsilon O}$, then $U|\psi\rangle = e^{i\epsilon\phi}|\psi\rangle$. After absorbing the phase factor into the definition of O, i.e., $O \to O - \phi I$, we have $e^{i\epsilon O}|\psi\rangle = |\psi\rangle$, and its linearization gives

$$O|\psi\rangle = 0, \tag{1}$$

or $\langle\psi|O^\dagger O|\psi\rangle = 0$. For an internal symmetry with local generators, $O = \sum_n e^{ipn} G_{n,\ldots,n+N-1}$, where p is the momentum and $G_{n,\ldots,n+N-1}$ is an N-site operator starting at the nth site. Given a state $|\psi\rangle$ and a momentum p, if we aim to obtain an exact or approximate conserved quantity of this form which the state has, we can consider the optimization problem,

$$\min_G f(G, G^\dagger) = \min_G \frac{\langle\psi|O^\dagger O|\psi\rangle}{V\mathrm{Tr}[G^\dagger G]}, \tag{2}$$

with the normalization constraint $\|G\|^2 = \mathrm{Tr}[G^\dagger G] = 1$, where V is the system size. Note that this cost function has a physical interpretation of the static structure factor of G at momentum p. The unitarity of U requires O, and thus G, to be Hermitian. In that case, the optimum of f is reached when $\partial f/\partial G = 0$, i.e.,

$$\langle\psi|\frac{\partial O^\dagger}{\partial G}O|\psi\rangle + \langle\psi|O^\dagger\frac{\partial O}{\partial G}|\psi\rangle = 2\frac{\langle\psi|O^\dagger O|\psi\rangle}{\mathrm{Tr}[G^2]}G, \tag{3}$$

which, after vectorizing $G \mapsto \mathbf{g}$, becomes an eigenvalue problem,

$$(\mathcal{F} + \mathcal{F}^T)\cdot\mathbf{g} = 2\lambda_{\min}\mathbf{g}, \tag{4}$$

where the eigenvalues are guaranteed to be non-negative real numbers due to the positive semidefinite quadratic form of the cost function f, and it can be proved [21] that the eigenvectors G are guaranteed to be Hermitian up to an arbitrary overall phase. For an eigenvector G, the associated eigenvalue λ naturally measures how accurate the corresponding symmetry is.

For an infinite matrix product state (MPS) $|\psi\rangle$, this eigenvalue problem can be solved by adapting MPS techniques used in other contexts; readers not interested in these details can skip this paragraph. Take $|\psi\rangle$ as an infinite uniform MPS with one-site unit cell parametrized by tensors A_L, A_R, and A_C in the mixed gauge. The application of $\mathcal{F}$ to $\mathbf{g}$, and similarly $\mathcal{F}^T\cdot\mathbf{g}$, can be implemented by observing that [22] it is the same as calculating the static structure factor of G except that a hole is dug in all the terms, i.e.,

$$\mathcal{F}\cdot\mathbf{g} = \langle\psi|\frac{\partial O^\dagger}{\partial G}O|\psi\rangle$$

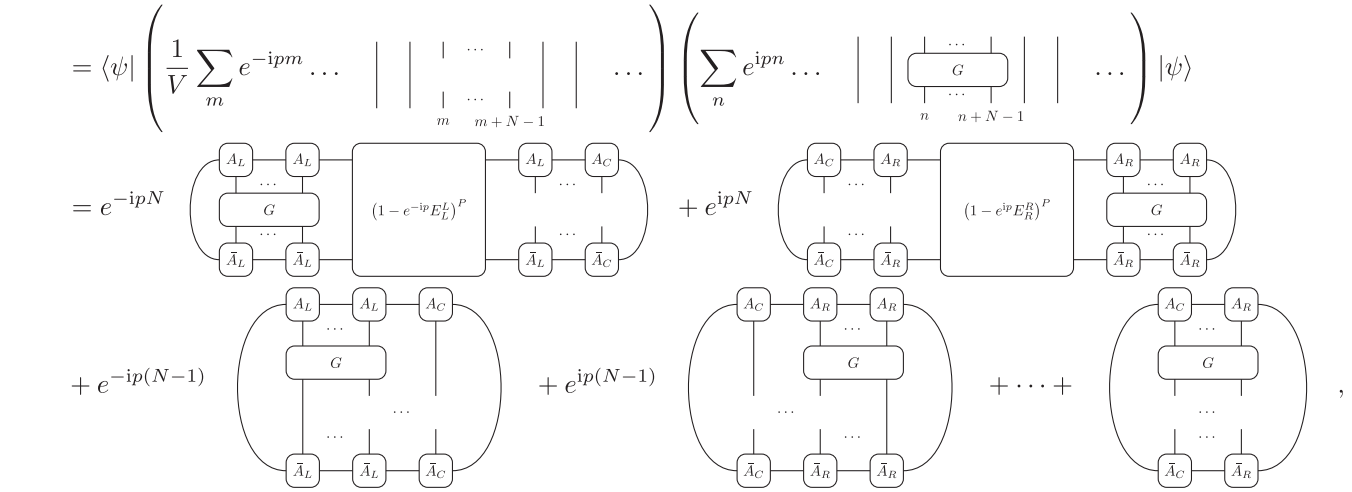

(5)

where the last "$\cdots$" means sum over all diagrams with $1 \le |n-m| \le N-2$, E_L^L and E_R^R are the left- and right-gauge MPS transfer matrices, and $(\cdot)^P$ denotes the pseudo-inverse resulting from the infinite geometric series [20] of all relative positions between G and the hole without overlap, which includes a regularization procedure effectively removing the disconnected part of the correlation functions and thus is automatically consistent with the phase factor absorption mentioned previously. We can then use an iterative eigensolver [23] to obtain the lowest several solutions [24].

In principle, the algorithm works for any MPS [25]. Particularly, we are interested in applying it to the variational uniform MPS [19] approximation of the gapless ground state of 1D critical Hamiltonians. Since a MPS with finite bond dimension is always gapped [20], it can never exactly represent a critical ground state of infinite correlation length and thus can never exactly capture the symmetry of a critical lattice Hamiltonian or of its low-energy effective field theory in the infrared limit. However, we may use the principle of entanglement scaling [26–28] and treat the finite bond dimension χ as a relevant perturbation, which enables us to identify the exact or emergent symmetries exclusively from the MPS through an extrapolation in the correlation length ξ, as shown by the benchmark results below.

Benchmarks for exact symmetries.—As a warming up, we first consider a critical model whose ground state has an exact U(1) symmetry [29]—the spin-1/2 isotropic quantum XY chain,

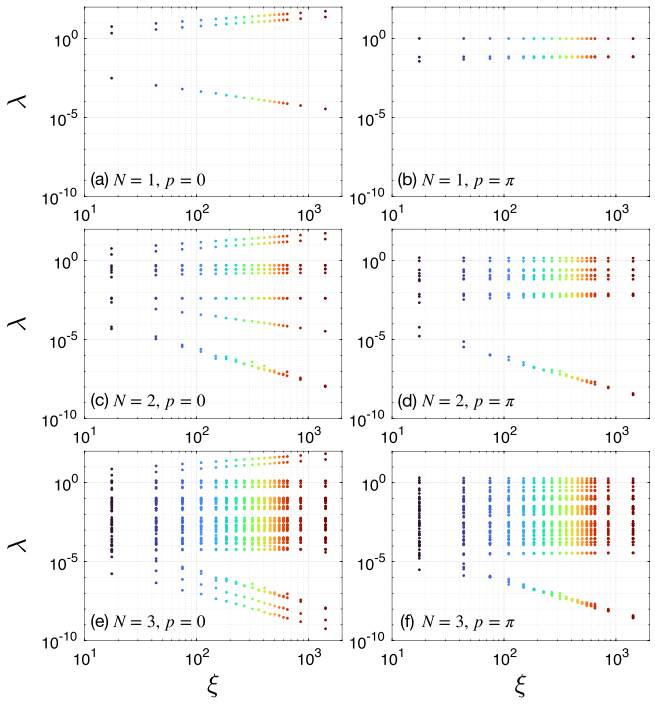

FIG. 1. Log-log plot of the eigenvalue spectrum of $\frac{1}{2}(\mathcal{F}+\mathcal{F}^T)$ versus the correlation length ξ for the spin-1/2 isotropic quantum XY chain. The correlation length of a MPS with a certain bond dimension is calculated by Eq. (40) in Ref. [20]. Note that in (e) there is one decaying λ hidden in the bulk of larger eigenvalues, but it becomes visible at larger correlation lengths.

$$H = -\sum_n (X_n X_{n+1} + Y_n Y_{n+1}), \tag{6}$$

where X_n, Y_n, and Z_n are the Pauli matrices at site n. The U(1) symmetry is generated by $O = \sum_n Z_n$ that satisfies $[H, \sum_n Z_n] = 0$. The model is integrable and thus has infinitely many local conserved quantities in the thermodynamic limit [30–33]. The critical low-energy physics is described [34] by the $\mathrm{U}(1)_4$ CFT of free bosons with central charge $c = 1$.

Applying our algorithm to MPS of various bond dimensions yields the local conserved quantities up to $N = 3$. The full spectrum (after removing the trivial solutions) of the eigenvalue problem in Eq. (4) is shown in Fig. 1 and the eigenvectors G associated with the decaying eigenvalues are shown in Table I. For $p = 0$, there are 1, 3, 5 eigenvalues decaying with the correlation length for $N = 1$, 2, 3, respectively; for $p = \pi$, there are 0, 2, 4 eigenvalues decaying with the correlation length for $N = 1$, 2, 3, respectively. The eigenvector $G = XX + YY$ corresponds to the Hamiltonian in Eq. (6), so as a by-product our method is also able to determine the local parent Hamiltonian [35–37] solely from its ground state. We notice that the decay has a power-law scaling $\lambda \sim \xi^{-\eta'}$ [38]; the exponents are listed in Table I. All other eigenvalues increase or stay constant with the increasing correlation length. The G's associated with the decaying λ's are local integrals of motion since λ is extrapolated to 0 at infinite correlation length. While the conserved quantities in Table I and more conserved quantities for larger N in the XY model can be constructed recursively [21] through the master symmetry approach [6,30–32,39], our method provides an alternative way to obtain them generally.

TABLE I. Local conserved quantities in the spin-1/2 isotropic quantum XY chain up to $N = 3$. Smaller-N solutions reappear at larger N, and we only show the new solutions at each N. The η' is obtained from the scaling of $\langle\psi|O^\dagger O|\psi\rangle$ with ξ, which is slightly different from the slope of the decaying eigenvalues in Fig. 1, since different solutions can mix with each other and their form also become more accurate as ξ increases.

p	N	G	η'
0	1	Z	1.009
	2	$XX + YY$	1.985
		$XY - YX$	1.933
	3	$XZX + YZY$	1.008
		$XZY - YZX$	1.939
π	1	...	...
	2	$XX - YY$	2.005
		$XY + YX$	2.008
	3	$XZX - YZY$	2.046
		$XZY + YZX$	2.063

Extended symmetries by emergent symmetries.—The ground state of the spin-1/2 antiferromagnetic Heisenberg chain is expected to have an emergent symmetry in addition to the microscopic SU(2) symmetry of the lattice Hamiltonian, and thus the symmetry is extended to $\mathrm{SO}(4) = [\mathrm{SU}(2)_L \times \mathrm{SU}(2)_R]/Z_2$ [5,40]. Here, we consider the J-Q model [7]—a modified Heisenberg chain at whose transition point still exists the extended symmetry:

$$H = -J\sum_n P_{n,n+1} - Q\sum_n P_{n,n+1}P_{n+2,n+3}, \tag{7}$$

where $P_{n,n+1} = 1/4 - \mathbf{S}_n \cdot \mathbf{S}_{n+1}$, with $\mathbf{S}_n = (S_n^x, S_n^y, S_n^z) = \frac{1}{2}(X_n, Y_n, Z_n)$. The dimer order enforced by strong four-site interaction transits to a critical phase when $Q/J \lesssim 0.848\,31$ [41,42], at which [43] the effective description is the $c = 1$ $\mathrm{SU}(2)_1$ Wess-Zumino-Witten CFT [5,40].

Figure 2 shows the eigenvalues of our optimization problem after imposing the time reversal, parity, and spin-flip symmetries [21] of the microscopic Hamiltonian at the transition point. The eigenvectors associated with all the eigenvalues shown in Fig. 2 except the faded ones are lattice operator approximation for the conserved currents of the extended symmetry to different precision, which could be confirmed by checking [21] that their scaling dimension is one [5]. To identify the eigenvalues that associate with the same G's at different ξ, we search for the eigenvectors at smaller ξ's which have the largest overlap with each of

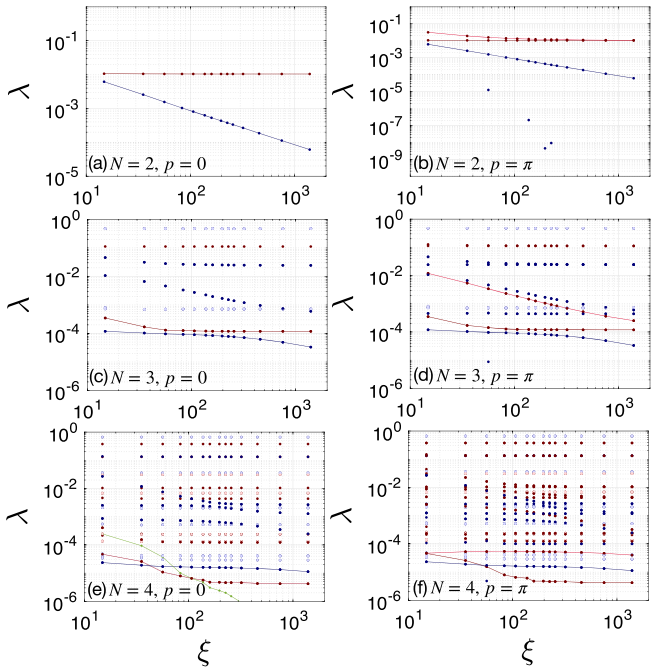

FIG. 2. Eigenvalue spectrum for the spin-1/2 J-Q Heisenberg model after imposing microscopic symmetries. The G's associated with the blue (red) dots are parity even (odd) and time reversal odd (even). The scaling dimension of the G associated with the faded dots is not one, and thus they are not emergent continuous internal symmetries. The green curve in (e) corresponds to the Hamiltonian. Note that in (d) and (f) one solution corresponding to one of the three generators for the exact SU(2) symmetry of the microscopic Hamiltonian is not shown since it is well below 10^{-6}. We use a sublattice rotation about the z axis by angle π when using variational uniform MPS to optimize the ground state, so the x and y components of the generators move to $p = \pi$.

the lowest several eigenvectors at the largest ξ reached, as tracked by the colored lines in Fig. 2. The dots connected by blue and red lines at the bottom of the spectrum are the best approximation among all of the solutions. Different from the exact symmetries, eigenvalues corresponding to the emergent symmetries will finally saturate at some correlation length, because it is only an N-site truncated approximation of the exact emergent lattice generator.

We observe that three approximately conserved charges (red curves in Fig. 2), $M^\alpha = \sum_n m_n^\alpha$ ($\alpha \in \{x, y, z\}$), coming from the emergent symmetries, begin to appear at $N = 2$ in addition to the three exact microscopic SU(2) symmetry generators (blue curves in Fig. 2) $Q^\alpha = \sum_n S_n^\alpha$, and they become more conserved as N increases, which is obvious from the drop of the corresponding eigenvalues. At $N = 2$, $m_{n,\alpha} = \epsilon_{\alpha\beta\gamma} S_n^\beta S_{n+1}^\gamma$, with $\epsilon_{\alpha\beta\gamma}$ the Levi-Civita symbol; at $N = 3$, the next-nearest neighbor term shows up and we have $m_{n,\alpha} = \epsilon_{\alpha\beta\gamma}(w_1 S_n^\beta S_{n+1}^\gamma + w_2 S_n^\beta S_{n+2}^\gamma)$, with $w_2/w_1 \approx 0.2253$ [45]. The form of the three-site $m_{n,\alpha}$ looks very similar to the level-1 Yangian [46–48]—which are exact conserved quantities of the RG fixed point, the Haldane-Shastry model [44,49]—truncated to the next-nearest neighbor coupling, though with different coupling coefficients [21]. When going to $N = 4$, the contribution from longer-range coupling in the level-1 Yangian appears with all coupling coefficients modified. Moreover, terms from the level-3 Yangian begin to be involved. We get $m_{n,\alpha} = m^1_{n,\alpha} + m^3_{n,\alpha}$, where $m^1_{n,\alpha} = \epsilon_{\alpha\beta\gamma}(w_1 S_n^\beta S_{n+1}^\gamma + w_2 S_n^\beta S_{n+2}^\gamma + w_3 S_n^\beta S_{n+3}^\gamma)$ and $m^3_{n,\alpha} = \epsilon_{\alpha\beta\gamma}[u_1 S_n^\beta S_{n+3}^\gamma \mathbf{S}_{n+1} \cdot \mathbf{S}_{n+2} + u_2 \mathbf{S}_n \cdot \mathbf{S}_{n+3} S_{n+1}^\beta S_{n+2}^\gamma + u_3(S_n^\beta S_{n+1}^\gamma \mathbf{S}_{n+2} \cdot \mathbf{S}_{n+3} + \mathbf{S}_n \cdot \mathbf{S}_{n+1} S_{n+2}^\beta S_{n+3}^\gamma) + u_4(S_n^\beta S_{n+2}^\gamma \mathbf{S}_{n+1} \cdot \mathbf{S}_{n+3} + \mathbf{S}_n \cdot \mathbf{S}_{n+2} S_{n+1}^\beta S_{n+3}^\gamma)]$, with $w_2/w_1 \approx 0.3557$, $w_3/w_1 \approx 0.1467$, $u_1/w_1 \approx 0.1577$, $u_2/w_1 \approx -0.09690$, $u_3/w_1 \approx -0.09141$, and $u_4/w_1 \approx 0.08169$. Considering that it is even under time reversal and odd under parity, $M^\alpha \sim J_0^\alpha - \bar{J}_0^\alpha$, where J_0^α ($\bar{J}_0^\alpha$) is the zero mode of the Kac-Moody generators, which form the ordinary Lie algebra $\mathfrak{su}(2)_L$ [$\mathfrak{su}(2)_R$] [50]. Since $Q^\alpha \sim J_0^\alpha + \bar{J}_0^\alpha$ [51], M^α and Q^α can then be linearly combined to construct J_0^α and $\bar{J}_0^\alpha$, and other modes of the Kac-Moody generators can be constructed by the Fourier transform of the currents [6].

Emergent symmetries at a DQCP.—The following spin-1/2 chain, studied by Jiang and Motrunich [52],

$$H = \sum_n (-J_x X_n X_{n+1} - J_z Z_n Z_{n+1}) + \sum_n (K_{2x} X_n X_{n+2} + K_{2z} Z_n Z_{n+2}), \tag{8}$$

has an on-site $Z_2 \times Z_2$ spin flip. It undergoes a direct continuous transition from a valence bond solid to ferromagnetic order at $K_{2x} = K_{2z} = 1/2$, $J_x = 1$, $J_z \approx 1.4645$ [8], which has been proposed to be a DQCP with an emergent $\mathrm{U}(1) \times \mathrm{U}(1)$ symmetry [8,53] that is also generated by the zero modes of the Kac-Moody algebra.

Applying our algorithm to the critical point, we find a single solution $G = Z$ for $N = 1$. From $N = 2$, we require the eigenvectors to transform the same as Z under the spin-flip symmetry when solving the eigenvalue problem, and find two solutions at $p = \pi$ as shown in Figs. 3(a)–3(c). For $N = 2$, the lowest solution (blue) is $G_1 = ZI - IZ$ (i.e., a staggered Z), and the second solution (red) is $G_2 = XY + YX$, which satisfies $[G_1, G_2] = 0$; these are indeed precisely the same effective lattice operators identified as conserved currents for the emergent $\mathrm{U}(1) \times \mathrm{U}(1)$ through bosonization [8]. At $N = 3$, the corresponding eigenvalues for G_1 and G_2 improve by almost 1 and 2 orders of magnitude, respectively. The form of both solutions modifies significantly by three-site terms as compared to $N = 2$—and thus compared to the field theory prediction—G_1 becomes $(v_1/3)(-ZII + IZI - IIZ) + v_2 ZZZ + v_3(YYZ + ZYY) + v_4(XXZ + ZXX) + v_5 XZX + v_6 YZY$, with $v_2/v_1 \approx 0.1615$, $v_3/v_1 \approx 0.0988$, $v_4/v_1 \approx 0.0882$, $v_5/v_1 \approx 0.0410$, and $v_6/v_1 \approx -0.1399$; G_2 becomes $w_1[(XY + YX)I - I(XY + YX)] + 2w_2(XIY - YIX)$, with

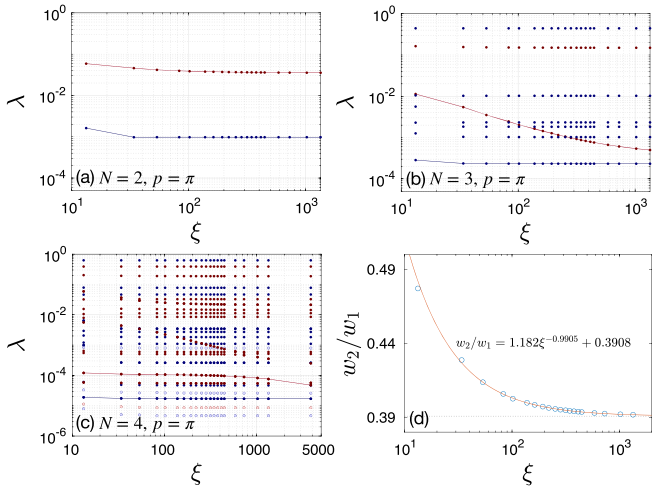

FIG. 3. Eigenvalue spectrum for the Jiang-Motrunich model after imposing microscopic symmetries at $p = \pi$ for (a) $N = 2$, (b) $N = 3$, and (c) $N = 4$. The color convention is the same as in Fig. 2. (d) The ratio between the coefficient in front of the nearest neighbor term and next-nearest neighbor term in G_2 at $N = 3$ [the red curve in (b)].

$w_2/w_1 \approx 0.3908$ [Fig. 3(d)]. When pushing to $N = 4$, longer-ranged terms further dress G_1 and G_2 [21]. Our algorithm hence allows us to decorate the bare form of the lattice operators for emergent symmetry generators found through field theory analysis, and therefore to obtain a more precise picture of the microscopic nature of the emergent symmetries.

Conclusions.—We have presented a novel general method to numerically detect emergent continuous internal symmetries in critical systems. The bottom line is that emergent symmetries do not just reveal themselves indirectly in the long-distance behavior of correlation functions—which has been the sole detection mechanism before our work—but are actually realized surprisingly accurately on the lattice, albeit with spatially extended generators. We have illustrated this by rediscovering the theory-predicted lattice operators for the emergent conserved currents at a 1D DQCP and sharply improving them with newly discovered correction terms. We have also identified the effective lattice operators of the conserved charges for the extended SO(4) symmetry in the J-Q chain with Yangian generators truncated to local terms, which were unknown before. The ability of our method to crack the explicit form of these lattice generators allows us to construct the emergent lattice Kac-Moody generators to unprecedented accuracy for both Abelian and non-Abelian symmetries [54] in generic settings.

Outlook.—This method could in principle be generalized to 2D, to extract emergent lattice conserved currents in the projected entangled pair states [55–57], which would be of particular use for the study of higher-dimensional DQCP. A variant version with a larger unit cell can be easily derived. It is also worth exploring if a similar algorithm works for finite systems with periodic or other boundary conditions, for the low-energy excited states [58], or for classical systems. Adjusting this method to find unconventional symmetries of the weakly entangled higher excited states [59,60] or the emergent space-time symmetry [61] would also be interesting directions.

The complexity of the eigenvalue problem scales exponentially with N. To reduce the complexity of solving for G of larger size, we could resort to the density matrix renormalization group [15,16] by treating G as an N-site finite matrix product operator (MPO) [62,63], and the tricky part will be removing the trivial solutions efficiently [21,24]. It would also be desirable to include terms with long-range tails by representing O as an infinite MPO [64], though its implementation encounters some technical difficulties [21].

We thank Frank Verstraete, Natalia Chepiga, Jutho Haegeman, Laurens Vanderstraeten, Wen-Tao Xu, András Molnár, Anna Francuz, Ilya Kull, José Garre Rubio, Juraj Hasik, Rui-Zhen Huang, Pranay Patil, and especially Hong-Hao Tu for illuminating discussions. We also acknowledge the hospitality of the Erwin Schrödinger International Institute for Mathematics and Physics (ESI) during the long-term program "Tensor Networks: Mathematical Structures and Novel Algorithms," which stimulated many of the discussions. This work has received support from the European Union's Horizon 2020 program through Grant No. 863476 (ERC-CoG SEQUAM). The tensor contractions are implemented using NCON [65]. The codes are available on github [66].

[1] T. Senthil, A. Vishwanath, L. Balents, S. Sachdev, and M. P. A. Fisher, Deconfined quantum critical points, Science **303**, 1490 (2004).
[2] T. Senthil, L. Balents, S. Sachdev, A. Vishwanath, and M. P. A. Fisher, Quantum criticality beyond the Landau-Ginzburg-Wilson paradigm, Phys. Rev. B **70**, 144407 (2004).
[3] P. Francesco, P. Mathieu, and D. Sénéchal, *Conformal Field Theory* (Springer, New York, 1997).
[4] P. Ginsparg, Applied Conformal Field Theory, arXiv:hep-th/9108028.
[5] I. Affleck, Critical Behavior of Two-Dimensional Systems with Continuous Symmetries, Phys. Rev. Lett. **55**, 1355 (1985).
[6] R. Wang, Y. Zou, and G. Vidal, Emergence of Kac-Moody symmetry in critical quantum spin chains, Phys. Rev. B **106**, 115111 (2022).
[7] P. Patil, E. Katz, and A. W. Sandvik, Numerical investigations of SO(4) emergent extended symmetry in spin-$\frac{1}{2}$ Heisenberg antiferromagnetic chains, Phys. Rev. B **98**, 014414 (2018).
[8] R.-Z. Huang, D.-C. Lu, Y.-Z. You, Z. Y. Meng, and T. Xiang, Emergent symmetry and conserved current at a one-dimensional incarnation of deconfined quantum critical point, Phys. Rev. B **100**, 125137 (2019).

[9] N. Ma, Y.-Z. You, and Z. Y. Meng, Role of Noether's Theorem at the Deconfined Quantum Critical Point, Phys. Rev. Lett. **122**, 175701 (2019).

[10] H. Dreyer, L. Vanderstraeten, J.-Y. Chen, R. Verresen, and N. Schuch, Robustness of critical U(1) spin liquids and emergent symmetries in tensor networks, arXiv:2008.04833.

[11] A. W. Sandvik, Evidence for Deconfined Quantum Criticality in a Two-Dimensional Heisenberg Model with Four-Spin Interactions, Phys. Rev. Lett. **98**, 227202 (2007).

[12] J. Y. Lee, J. Ramette, M. A. Metlitski, V. Vuletic, W. W. Ho, and S. Choi, Landau-Forbidden quantum criticality in Rydberg quantum simulators, arXiv:2207.08829.

[13] L. Wang and A. W. Sandvik, Critical Level Crossings and Gapless Spin Liquid in the Square-Lattice Spin-$1/2$ J_1–J_2 Heisenberg Antiferromagnet, Phys. Rev. Lett. **121**, 107202 (2018).

[14] M. Hermele, T. Senthil, and M. P. A. Fisher, Algebraic spin liquid as the mother of many competing orders, Phys. Rev. B **72**, 104404 (2005).

[15] S. R. White, Density Matrix Formulation for Quantum Renormalization Groups, Phys. Rev. Lett. **69**, 2863 (1992).

[16] S. R. White, Density-matrix algorithms for quantum renormalization groups, Phys. Rev. B **48**, 10345 (1993).

[17] R. Orús, Tensor networks for complex quantum systems, Nat. Rev. Phys. **1**, 538 (2019).

[18] J. I. Cirac, D. Pérez-García, N. Schuch, and F. Verstraete, Matrix product states and projected entangled pair states: Concepts, symmetries, theorems, Rev. Mod. Phys. **93**, 045003 (2021).

[19] V. Zauner-Stauber, L. Vanderstraeten, M. T. Fishman, F. Verstraete, and J. Haegeman, Variational optimization algorithms for uniform matrix product states, Phys. Rev. B **97**, 045145 (2018).

[20] L. Vanderstraeten, J. Haegeman, and F. Verstraete, Tangent-space methods for uniform matrix product states, SciPost Phys. Lect. Notes 7 (2019).

[21] See Supplemental Material at http://link.aps.org/supplemental/10.1103/PhysRevLett.131.036505 for more details.

[22] We adopt the same notation as in Ref. [20].

[23] Y. Saad, *Numerical Methods for Large Eigenvalue Problems* (Society for Industrial and Applied Mathematics, Philadelphia, 2011).

[24] Note that there always exist trivial solutions of the form $G = X \otimes I - I \otimes X$ for $p = 0$ and $G = X \otimes I + I \otimes X$ for $p = \pi$, with X being any $(N-1)$-site operator (except the identity) and I being the one-site identity. The N-site identity is also a trivial solution by regularization. The eigenvalues associated with those trivial solutions are exactly zero. In total they span a large trivial null space of dimension $d^{2(N-1)}$, where d is the dimension of the one-site physical Hilbert space. We have removed the trivial solutions from all of our results. See the Supplemental Material [21] for how to remove the trivial solutions.

[25] Solving the symmetry of the ground state of a gapped model is much easier, and another method based on the MPS fundamental theorem also works [21].

[26] L. Tagliacozzo, T. R. de Oliveira, S. Iblisdir, and J. I. Latorre, Scaling of entanglement support for matrix product states, Phys. Rev. B **78**, 024410 (2008).

[27] F. Pollmann, S. Mukerjee, A. M. Turner, and J. E. Moore, Theory of Finite-Entanglement Scaling at One-Dimensional Quantum Critical Points, Phys. Rev. Lett. **102**, 255701 (2009).

[28] M. M. Rams, P. Czarnik, and L. Cincio, Precise Extrapolation of the Correlation Function Asymptotics in Uniform Tensor Network States with Application to the Bose-Hubbard and XXZ Models, Phys. Rev. X **8**, 041033 (2018).

[29] In fact, the symmetry should be $\mathrm{U}(1) \times \mathrm{U}(1)$. See Ref. [5].

[30] E. Barouch and B. Fuchssteiner, Master symmetries and similarity equations of the XYh model, Stud. Appl. Math. **73**, 221 (1985).

[31] H. Araki, Master symmetries of the XY model, Commun. Math. Phys. **132**, 155 (1990).

[32] T. Matsui, On conservation laws of the XY model, in *Quantum and Non-Commutative Analysis: Past, Present and Future Perspectives*, edited by H. Araki, K. R. Ito, A. Kishimoto, and I. Ojima (Springer Netherlands, Dordrecht, 1993), pp. 197–204.

[33] M. Fagotti, Local conservation laws in spin-$1/2$ XY chains with open boundary conditions, J. Stat. Mech. (2016) 063105.

[34] H.-H. Tu, Universal Entropy of Conformal Critical Theories on a Klein Bottle, Phys. Rev. Lett. **119**, 261603 (2017).

[35] J. R. Garrison and T. Grover, Does a Single Eigenstate Encode the Full Hamiltonian?, Phys. Rev. X **8**, 021026 (2018).

[36] X.-L. Qi and D. Ranard, Determining a local Hamiltonian from a single eigenstate, Quantum **3**, 159 (2019).

[37] E. Chertkov and B. K. Clark, Computational Inverse Method for Constructing Spaces of Quantum Models from Wave Functions, Phys. Rev. X **8**, 031029 (2018).

[38] Depending on the quantum number the operator carries, the correlation length of correlation functions of an operator can be different from the correlation length of the MPS [21]. It turns out that the critical exponents here have no universal relation to the scaling dimension of the corresponding operator [21].

[39] K. Sogo and M. Wadati, Boost operator and its application to quantum Gelfand-Levitan equation for Heisenberg-Ising chain with spin one-half, Prog. Theor. Phys. **69**, 431 (1983).

[40] I. Affleck and F. D. M. Haldane, Critical theory of quantum spin chains, Phys. Rev. B **36**, 5291 (1987).

[41] Y. Tang and A. W. Sandvik, Method to Characterize Spinons as Emergent Elementary Particles, Phys. Rev. Lett. **107**, 157201 (2011).

[42] S. Sanyal, A. Banerjee, and K. Damle, Vacancy-induced spin texture in a one-dimensional $S = \frac{1}{2}$ Heisenberg antiferromagnet, Phys. Rev. B **84**, 235129 (2011).

[43] The marginally irrelevant spin-umklapp term which introduces a logarithmic correction to the correlation function vanishes at the transition point, like in the J_1-J_2 model [7,44].

[44] F. D. M. Haldane, Exact Jastrow-Gutzwiller Resonating-Valence-Bond Ground State of the Spin-$\frac{1}{2}$ Antiferromagnetic Heisenberg Chain with $1/r^2$ Exchange, Phys. Rev. Lett. **60**, 635 (1988).

[45] This form of the three-site $m_{n,\alpha}$ and the ratio w_2/w_1 in the J-Q model are very similar to those in the J_1-J_2 model [6]. They flow to the same RG fixed point and they are very

similar even on the lattice level. To check this, we have performed exact diagonalization of a system size of 18 sites and found that the fidelity between their ground states is 0.9987.

[46] F. D. M. Haldane, Z. N. C. Ha, J. C. Talstra, D. Bernard, and V. Pasquier, Yangian Symmetry of Integrable Quantum Chains with Long-Range Interactions and a New Description of States in Conformal Field Theory, Phys. Rev. Lett. **69**, 2021 (1992).

[47] J. C. Talstra and F. D. M. Haldane, Integrals of motion of the Haldane-Shastry model, J. Phys. A **28**, 2369 (1995).

[48] V. Drinfeld, Hopf algebras and the quantum Yang-Baxter equation, Dokl. Akad. Nauk SSSR **283**, 1060 (1985).

[49] B. S. Shastry, Exact Solution of an $S = 1/2$ Heisenberg Antiferromagnetic Chain with Long-Ranged Interactions, Phys. Rev. Lett. **60**, 639 (1988).

[50] Note that $J_\alpha + \bar{J}_\alpha$ also satisfies the $\mathfrak{su}(2)$ algebra, but $J_\alpha - \bar{J}_\alpha$ does not.

[51] Strictly speaking, from bosonization [5] one knows that $S^\alpha(x) \sim [J_0^\alpha(x) + \bar{J}_0^\alpha(x)] + (-1)^x$ (term with scaling dimension $1/2$); however, the latter staggered part would cancel out upon sum over x and we get only $J_0^\alpha + \bar{J}_0^\alpha$.

[52] S. Jiang and O. Motrunich, Ising ferromagnet to valence bond solid transition in a one-dimensional spin chain: Analogies to deconfined quantum critical points, Phys. Rev. B **99**, 075103 (2019).

[53] B. Roberts, S. Jiang, and O. I. Motrunich, Deconfined quantum critical point in one dimension, Phys. Rev. B **99**, 165143 (2019).

[54] Note that it happened to be easy to tell what symmetry group the lattice generators obey in the above examples. Had this not been the case we would have had to study the commutation relations of the generators projected onto the low-energy sector to discover the algebra.

[55] F. Verstraete and J. I. Cirac, Renormalization algorithms for quantum-many body systems in two and higher dimensions, arXiv:cond-mat/0407066.

[56] L. Vanderstraeten, M. Mariën, F. Verstraete, and J. Haegeman, Excitations and the tangent space of projected entangled-pair states, Phys. Rev. B **92**, 201111(R) (2015).

[57] L. Vanderstraeten, J. Haegeman, and F. Verstraete, Simulating excitation spectra with projected entangled-pair states, Phys. Rev. B **99**, 165121 (2019).

[58] J. Haegeman, B. Pirvu, D. J. Weir, J. I. Cirac, T. J. Osborne, H. Verschelde, and F. Verstraete, Variational matrix product ansatz for dispersion relations, Phys. Rev. B **85**, 100408(R) (2012).

[59] M. Serbyn, Z. Papić, and D. A. Abanin, Local Conservation Laws and the Structure of the Many-Body Localized States, Phys. Rev. Lett. **111**, 127201 (2013).

[60] S. Moudgalya and O. I. Motrunich, Numerical methods for detecting symmetries and commutant algebras, Phys. Rev. B **107**, 224312 (2023).

[61] T.-C. Lin and J. McGreevy, Conformal field theory ground states as critical points of an entropy function, arXiv:2303.05444.

[62] G. M. Crosswhite and D. Bacon, Finite automata for caching in matrix product algorithms, Phys. Rev. A **78**, 012356 (2008).

[63] G. M. Crosswhite, A. C. Doherty, and G. Vidal, Applying matrix product operators to model systems with long-range interactions, Phys. Rev. B **78**, 035116 (2008).

[64] D. E. Parker, X. Cao, and M. P. Zaletel, Local matrix product operators: Canonical form, compression, and control theory, Phys. Rev. B **102**, 035147 (2020).

[65] R. N. C. Pfeifer, G. Evenbly, S. Singh, and G. Vidal, NCON: A tensor network contractor for MATLAB, arXiv:1402.0939.

[66] M. Yang, Emergent Symmetry (2023), 10.5281/zenodo.8115408.